ULTRA SONO GRAPHY

Microflow imaging versus color Doppler imaging for differentiating malignant from non-neoplastic peripheral lung lesions

Mustafa Yeşilyurt[1], Ahmet Tuğrul Akkuş[1], Buğra Kerget[2], Fahri Aydin[1], Adem Karaman[1], Fatih Alper[1]

[1]Department of Radiology, Faculty of Medicine, Atatürk University, Erzurum; [2]Department of Pulmonary Medicine, Faculty of Medicine, Atatürk University, Erzurum, Turkey

ORIGINAL ARTICLE

https://doi.org/10.14366/usg.26073
eISSN: 2288-5943
Ultrasonography 2026;45:587-594

Received: February 18, 2026
Revised: July 14, 2026
Accepted: August 4, 2026

Correspondence to:
Mustafa Yeşilyurt, MD, Department of Radiology, Faculty of Medicine, Atatürk University, 25040 Erzurum, Turkey
Tel. +90-442-344-6920
Fax. +90-442-2361014
E-mail: drmyesilyurt@gmail.com

Purpose: This study aimed to compare microflow imaging (MFI) with conventional color Doppler imaging (CDI) for differentiating malignant from non-neoplastic peripheral lung lesions on the basis of vascular grading and vascular morphology.

Methods: This retrospective single-center study included 124 patients with pleura-based peripheral lung lesions who underwent thoracic ultrasound between January 2024 and January 2026. Each lesion was examined with B-mode ultrasound, CDI, and MFI during the same session. Vascularity was graded according to the Adler classification, and vascular morphology was assigned to one of five predefined patterns. Histopathological findings or clinical and radiological follow-up served as the reference standard. Receiver operating characteristic curve analysis and multivariable logistic regression were performed.

Results: Among the 124 lesions, 77 (62.1%) were malignant and 47 (37.9%) were non-neoplastic. Vascularity scores obtained with both MFI and CDI were significantly higher in malignant lesions than in non-neoplastic lesions (P<0.001). The MFI morphology score achieved the highest diagnostic performance (area under the curve [AUC], 0.933; 95% confidence interval [CI], 0.888 to 0.979), followed by the MFI Adler score (AUC, 0.899), CDI Adler score (AUC, 0.847), and CDI morphology score (AUC, 0.828). At a cutoff of ≥3, the MFI morphology score yielded 94% sensitivity and 83% specificity. In multivariable analysis, only the MFI morphology score remained an independent predictor of malignancy (odds ratio, 6.13; 95% CI, 2.02 to 18.56; P=0.001).

Conclusion: MFI, particularly vascular morphology assessment, showed better diagnostic performance than CDI for differentiating malignant from non-neoplastic peripheral lung lesions and may improve routine thoracic ultrasound evaluation.

Keywords: Ultrasonography; Lung neoplasms; Doppler ultrasonography; Angiogenesis; Diagnostic imaging

Key points: Microflow imaging morphology showed better diagnostic performance than conventional color Doppler imaging for differentiating malignant from non-neoplastic peripheral lung lesions. Higher microflow morphology scores were an independent predictor of malignancy and showed excellent diagnostic accuracy. Adding microvascular morphology assessment to routine thoracic ultrasound may improve risk stratification and support biopsy decision-making in pleura-based lung lesions.

This is an Open Access article distributed under the terms of the Creative Commons Attribution Non-Commercial License (http://creativecommons.org/licenses/by-nc/4.0/) which permits unrestricted noncommercial use, distribution, and reproduction in any medium, provided the original work is properly cited.

Copyright © 2026 Korean Society of Ultrasound in Medicine (KSUM)

How to cite this article:
Yeşilyurt M, Akkuş AT, Kerget B, Aydin F, Karaman A, Alper F. Microflow imaging versus color Doppler imaging for differentiating malignant from non-neoplastic peripheral lung lesions. Ultrasonography 2026;45:587-594.

Introduction

Peripheral lung lesions include a broad range of pathological entities, from benign inflammatory or infectious processes to primary lung malignancies and metastatic disease [1]. Distinguishing non-neoplastic from malignant lesions is essential for guiding clinical management and avoiding unnecessary invasive procedures. However, conventional imaging modalities, including computed tomography, may show overlapping morphological features, particularly in pleura-based lesions that are accessible to ultrasound evaluation [2].

Thoracic ultrasound is increasingly used as an adjunctive modality for assessing peripheral lung lesions. It provides real-time imaging without ionizing radiation and permits direct visualization of pleura-based abnormalities [2]. In addition to structural assessment, Doppler ultrasound can provide functional information by depicting intralesional and perilesional vascularity, which may reflect tumor angiogenesis and biological behavior. Malignant lesions generally show increased, irregular, and chaotic vascular patterns, whereas non-neoplastic lesions more often show absent or organized vascular signals [3].

Despite these advantages, conventional color Doppler imaging (CDI) has limited sensitivity for low-velocity and microvascular blood flow because motion artifacts and filtering algorithms can suppress slow-flow signals [3]. As a result, subtle microvascular structures may be missed, which can reduce diagnostic accuracy. These limitations are largely attributable to conventional wall-filtering and motion-suppression algorithms, which may remove slow-flow microvascular signals together with tissue-motion artifacts. This technical constraint may be especially important in thoracic applications, where respiratory motion and lesion depth can further reduce Doppler sensitivity.

Microflow imaging (MFI) is an advanced Doppler technique that uses adaptive clutter-suppression algorithms to improve real-time visualization of low-velocity microvascular flow without contrast agents [4]. These adaptive spatiotemporal algorithms help separate low-velocity flow from background tissue motion while preserving real-time imaging. Studies of several organs, including the breast, thyroid, lymph nodes, and kidney, have shown that MFI improves microvascular detection and delineates vascular morphology more clearly than conventional CDI [4–6].

However, data on the use of MFI in thoracic lesions remain scarce, and conventional CDI and MFI have not yet been systematically compared head-to-head in peripheral lung lesions.

Although contrast-enhanced ultrasound (CEUS) has been used to evaluate the perfusion characteristics of lung lesions [7], it is a distinct imaging modality with specific indications, higher cost, and limited availability in routine clinical practice. Therefore, optimizing non-contrast Doppler techniques that can be integrated seamlessly into routine thoracic ultrasound examinations remains clinically relevant.

Therefore, this study aimed to compare conventional CDI and MFI for evaluating vascularity and vascular morphology in peripheral lung lesions, using histopathological findings and clinical follow-up as the reference standard. By applying established semiquantitative vascular grading and vascular morphology classifications, this study sought to determine whether MFI provides incremental diagnostic value over CDI for differentiating malignant from non-neoplastic peripheral lung lesions. It was hypothesized that MFI would show higher vascular grades and more complex vascular morphology in malignant lesions than conventional CDI, thereby improving diagnostic discrimination.

Materials and Methods

Compliance with Ethical Standards

This study was approved by the Institutional Review Board of Atatürk University (Meeting No. 01, Decision No. 10, January 30, 2026). Informed consent was waived due to the retrospective nature of the study. The study followed the principles of the Declaration of Helsinki.

Study Design and Patient Population

Thoracic ultrasound examinations performed between January 2024 and January 2026 were reviewed retrospectively. All consecutive eligible patients during the study period were included to minimize potential selection bias. Patients with peripheral lung lesions were screened for eligibility. Eligible cases included patients with either pleura-based solid masses suspicious for malignancy or infectious/inflammatory consolidations in which a neoplastic lesion could not be reliably excluded on initial imaging.

Peripheral lung lesions were defined as solid or consolidation-type lesions that abutted, or were immediately adjacent to, the pleura without intervening aerated lung parenchyma, thereby allowing direct ultrasound evaluation.

A total of 151 consecutive patients met the initial screening criteria. Of these, 27 patients were excluded from the final analysis: 19 because they lacked a definitive pathological or clinical diagnosis, five because image quality was inadequate owing to motion artifacts or a poor acoustic window, and three because Doppler datasets were incomplete, with either CDI or MFI absent. The patient selection process is shown in Fig. 1.

After exclusions, 124 patients were included in the final analysis: 77 with malignant lesions and 47 with non-neoplastic lesions.

Malignant lesions were confirmed by histopathological examination of specimens obtained through percutaneous biopsy or surgical

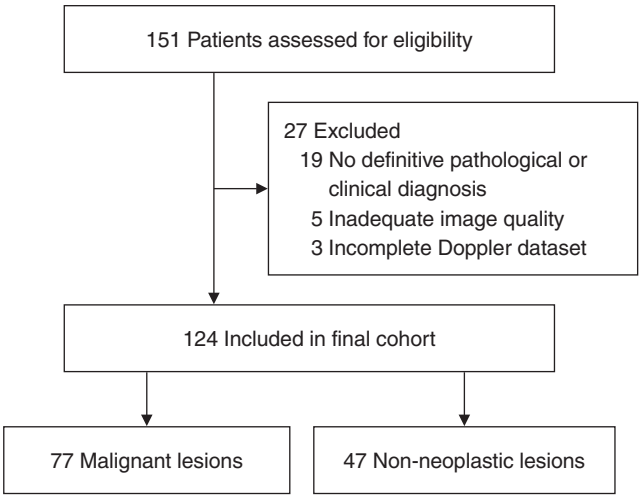


Fig. 1. Flow diagram of patient inclusion and exclusion in the study.

resection.

Non-neoplastic lesions were diagnosed either histopathologically or through clinical and radiological follow-up showing lesion resolution or long-term stability consistent with inflammatory, infectious, or fibrotic pathology. For cases diagnosed through follow-up, a minimum follow-up period of 6 months was required to support diagnostic reliability. Lesions were classified as non-neoplastic if they resolved completely, decreased substantially in size, or remained stable without progression during follow-up, together with clinical findings consistent with a non-neoplastic etiology. In this study, the comparator group consisted exclusively of non-neoplastic conditions and did not include benign neoplasms.

Ultrasound Examination Protocol

All ultrasound examinations were performed using a Philips EPIQ Elite ultrasound system (Philips Healthcare, Andover, MA, USA) equipped with a convex array transducer (2–5 MHz).

A radiologist with 8 years of experience in thoracic ultrasound acquired all scans during a single session. Use of one experienced operator promoted technical consistency across examinations, although it may limit external generalizability. At the time of examination, the operator was unaware of the final histopathological diagnosis but was aware of the clinical indication as part of routine practice.

B-mode ultrasound was first used to assess lesion size and general morphological appearance. The maximum lesion diameter was measured along the longest axis.

On the basis of B-mode appearance, lesions were classified as solid, mixed (containing both solid and cystic or necrotic components), or consolidation-like. Solid lesions were defined as discrete, predominantly homogeneous hypoechoic lesions without appreciable internal cystic or necrotic components. Mixed lesions were defined as lesions containing both solid tissue and internal cystic or necrotic components. Consolidation-like lesions were defined as subpleural hypoechoic areas with internal air and/or fluid bronchograms. CDI and MFI were then applied to evaluate intralesional vascularity.

During Doppler evaluation, the entire lesion was systematically scanned in multiple planes. The region with the greatest vascular signal within the lesion was identified, and representative still images and cine loops were archived for subsequent analysis.

For CDI, low-flow-optimized settings were applied, with a pulse repetition frequency (PRF) of 1680 Hz, a wall filter of 75 Hz, and a Doppler frequency of 3.5 MHz. For MFI, a dedicated microvascular preset was used, with a PRF of 250 Hz, a wall filter of 47 Hz, and a Doppler frequency of 3.0 MHz. These parameters were selected according to the manufacturer's recommendations to enhance slow-flow detection while minimizing motion-related artifacts. The same predefined presets were applied in all patients to standardize parameters across the study cohort. Doppler gain was adjusted just below the noise threshold (approximately 50%–52%) to minimize blooming artifacts while preserving true vascular signals.

Imaging depth and focal zone position were optimized according to lesion location but were kept consistent between CDI and MFI during the same examination session to permit direct intralesional comparison. To reduce respiratory-motion artifacts, patients were instructed to maintain shallow breathing during image acquisition. All Doppler assessments were performed consecutively during the same session to minimize physiological variability.

Power Doppler imaging was not included in the study protocol because the primary aim was to compare conventional CDI with MFI for microvascular assessment under routine clinical conditions.

Blood Flow Grading and Vascular Morphology Assessment

Tumor vascularity was assessed separately with CDI and MFI.

Blood flow was graded according to the semiquantitative method originally described by Adler et al. [8]: grade 0, No detectable intralesional vascular signal; grade 1, One or two dot-like or short linear vascular signals within the lesion; grade 2, Three to four dot-like vascular signals or one elongated intralesional vessel with a length approaching or exceeding the lesion radius; grade 3, More than five dot-like signals or two or more longer intralesional vessels.

Grading was performed independently for CDI and MFI. For each lesion, the highest vascular grade observed within the lesion was recorded for statistical analysis.

Vascular morphology was assessed separately for CDI and MFI using pattern-based criteria adapted from previously published microvascular imaging studies of solid tumors [9]. Because no standardized MFI morphology classification exists for peripheral lung lesions,

this categorization was applied in an exploratory manner. To minimize potential misclassification between preserved normal pulmonary vessels and tumor-related neoangiogenesis, the assessment focused on disorganized, tortuous, and irregular vascular patterns with chaotic branching or peripheral extension, rather than on regularly branching linear vessels consistent with normal pulmonary vascular architecture.

Vascular morphology was classified into five types: type I, no detectable vascular signal; type II, isolated dot-like intralesional signals; type III, short intralesional linear vessels without peripheral distribution; type IV, peripheral or rim-like vascular distribution; type V, disorganized or chaotic intralesional vascularity with perilesional extension.

Image Analysis

All ultrasound images were stored in the institutional archiving system and reviewed retrospectively.

Two radiologists with 8 and 12 years of experience in thoracic ultrasound, respectively, independently performed vascular grading (Adler score) and vascular morphology classification. Both readers were blinded to the final histopathological diagnosis, clinical follow-up results, and each other's assessments. CDI and MFI images were evaluated in separate reading sessions to minimize recall bias.

Grading and morphology assessments were performed separately for CDI and MFI. When readers disagreed, a consensus decision was reached after joint review, and consensus scores were used in the final diagnostic performance analysis.

Statistical Analysis

Statistical analyses were performed using IBM SPSS Statistics for Windows, version 27.0 (IBM Corp., Armonk, NY, USA). Continuous variables were expressed as medians (minimum–maximum), and categorical variables were presented as frequencies and percentages. Non-neoplastic and malignant lesions were compared using the Mann-Whitney U test for continuous variables and Pearson's chi-square test or Fisher's exact test for categorical variables, as appropriate.

Interobserver agreement for ordinal ultrasonographic parameters was evaluated using weighted Cohen's kappa statistics with linear weighting. This approach accounts for the degree of disagreement between ordinal categories. Kappa values were interpreted as follows: <0.20, poor; 0.21–0.40, fair; 0.41–0.60, moderate; 0.61–0.80, good; and >0.80, excellent agreement.

Receiver operating characteristic (ROC) curve analysis was performed to evaluate the diagnostic performance of ultrasonographic parameters for differentiating malignant from non-neoplastic lesions. The area under the curve (AUC), 95% confidence intervals (CIs), optimal cutoff values determined using the Youden index, sensitivity, and specificity were calculated. Pairwise comparisons between ROC curves were conducted using the DeLong method. In addition, the distribution of MFI morphology types I–V according to the final diagnosis was summarized in a cross-tabulation table (Supplementary Table 1), and the linear trend across morphology categories was evaluated using the linear-by-linear association test.

Multivariable binary logistic regression analysis was performed to identify independent predictors of malignancy. Potential multicollinearity among variables was assessed before variables were included in the multivariable model. Odds ratios (ORs) with 95% CIs were reported. A P-value <0.05 was considered statistically significant.

Results

A total of 124 patients were included in the final analysis: 77 with malignant lesions and 47 with non-neoplastic lesions. The median age of the overall cohort was 70 years (range, 40 to 88 years). The median age was 68 years (range, 40 to 86 years) among patients with non-neoplastic lesions and 72 years (range, 45 to 88 years) among those with malignant lesions; this difference was not statistically significant (P = 0.060). Overall, 89 patients (71.8%) were male.

Clinical and ultrasonographic characteristics of non-neoplastic and malignant lesions are summarized in Table 1. Upper-lobe localization

Table 1. Clinical and ultrasonographic characteristics of non-neoplastic and malignant lesions

Variable	Non-neoplastic (n = 47)	Malignant (n = 77)	P-value
Age (year)	68 (40–86)	72 (45–88)	0.060
Sex			0.540
Male	32 (68.1)	57 (74.0)	
Female	15 (31.9)	20 (26.0)	
Lesion localization			0.002
Left lower lobe	12 (25.5)	24 (31.2)	
Right lower lobe	20 (42.6)	9 (11.7)	
Left upper lobe	7 (14.9)	20 (26.0)	
Right upper lobe	7 (14.9)	23 (29.9)	
Right middle lobe	1 (2.1)	1 (1.3)	
Grayscale pattern			< 0.001
Solid	23 (48.9)	60 (77.9)	
Mixed (solid+necrotic)	9 (19.1)	16 (20.8)	
Consolidation-like	15 (31.9)	1 (1.3)	
Maximum lesion diameter (mm)	40 (16.6–128.9)	72 (22.2–137.1)	< 0.001
MFI Adler score	1 (0–3)	3 (1–3)	< 0.001
MFI morphology score	2 (1–5)	5 (2–5)	< 0.001
CDI Adler score	0 (0–3)	2 (0–3)	< 0.001
CDI morphology score	1 (1–3)	2 (1–5)	< 0.001

Values are presented as median (range) or number (%).
MFI, microflow imaging; CDI, color Doppler imaging.

was more frequent in malignant lesions, whereas right lower-lobe involvement was more common in non-neoplastic lesions (P = 0.002). In the grayscale assessment, malignant lesions were predominantly solid, whereas consolidation-like appearances were observed more frequently in non-neoplastic lesions (P < 0.001). Maximum lesion diameter was significantly larger in malignant lesions (P < 0.001). Doppler-based vascular grading and morphology scores obtained with MFI and CDI were significantly higher in malignant lesions than in non-neoplastic lesions (all P < 0.001).

The diagnostic distribution of lesions is presented in Table 2.

Interobserver agreement indicated good-to-excellent reliability across all ultrasonographic parameters. Weighted Cohen's kappa values were 0.763 (95% CI, 0.695 to 0.832) for the MFI Adler score, 0.810 (95% CI, 0.748 to 0.871) for the MFI morphology score, 0.821 (95% CI, 0.749 to 0.892) for the CDI Adler score, and 0.901 (95% CI, 0.845 to 0.956) for the CDI morphology score (all P < 0.001). Morphology-based scoring systems showed slightly higher interobserver agreement than vascular grading parameters.

Table 3 presents the multivariable logistic regression analysis for predicting malignancy. Among the evaluated Doppler parameters, only the MFI morphology score remained an independent predictor of malignancy (OR, 6.13; 95% CI, 2.02 to 18.56; P = 0.001). The MFI Adler score, CDI Adler score, and CDI morphology score were not independently associated with malignancy.

ROC curve analysis showed that all Doppler parameters significantly discriminated malignant from non-neoplastic lesions (all P < 0.001). Fig. 2 shows the ROC curves. Among the evaluated parameters, the MFI morphology score had the highest diagnostic performance (AUC, 0.933; 95% CI, 0.888 to 0.979), followed by the MFI Adler score (AUC, 0.899), CDI Adler score (AUC, 0.847), and CDI morphology score (AUC, 0.828). Table 4 summarizes the corresponding diagnostic performance metrics.

At an optimal cutoff of ≥ 3, the MFI morphology score yielded 94% sensitivity and 83% specificity. The MFI Adler score had similar sensitivity (94%) but lower specificity (75%) at a cutoff of ≥ 2. CDI Adler and CDI morphology scores showed lower diagnostic accuracy, with sensitivities of 88% and 86%, respectively, and specificities of 71% for both parameters at cutoffs of ≥ 1 and ≥ 2, respectively. Pairwise comparison using the DeLong method showed that the MFI morphology score performed significantly better than the CDI morphology score (AUC difference, 0.105; 95% CI, 0.047 to 0.163; z = 3.54; P < 0.001). Supplementary Table 1 presents the distribution of MFI morphology types I–V according to the final diagnosis. The proportion of malignant lesions increased progressively from type I (0.0%) to type V (97.9%), with a significant linear trend across morphology categories (linear-by-linear association $\chi^2 = 68.427$; P < 0.001).

Fig. 3 presents representative non-neoplastic and malignant cases with corresponding grayscale, CDI, and MFI findings.

Table 2. Diagnostic characteristics of the study population (n=124)

Diagnosis	No. (%)
Malignant lesions (n = 77)	
Adenocarcinoma	22 (28.6)
Squamous cell carcinoma	14 (18.2)
High-grade neuroendocrine carcinoma	12 (15.6)
Metastatic tumor	10 (13.0)
Non-small cell lung carcinoma, not otherwise specified	9 (11.7)
Non-epithelial malignant tumors[a]	10 (13.0)
Non-neoplastic lesions (n = 47)	
Non-neoplastic inflammatory/infectious lesions[b]	40 (85.1)
Fibrotic/reactive lung tissue	7 (14.9)

[a]Includes pleomorphic sarcoma, synovial sarcoma, undifferentiated small round cell sarcoma, diffuse large B-cell lymphoma, low-grade lymphoma, and plasma cell neoplasm. [b]Includes inflammatory/infectious lesions with and without necrotic consolidation.

Table 3. Multivariable logistic regression analysis for predicting malignancy

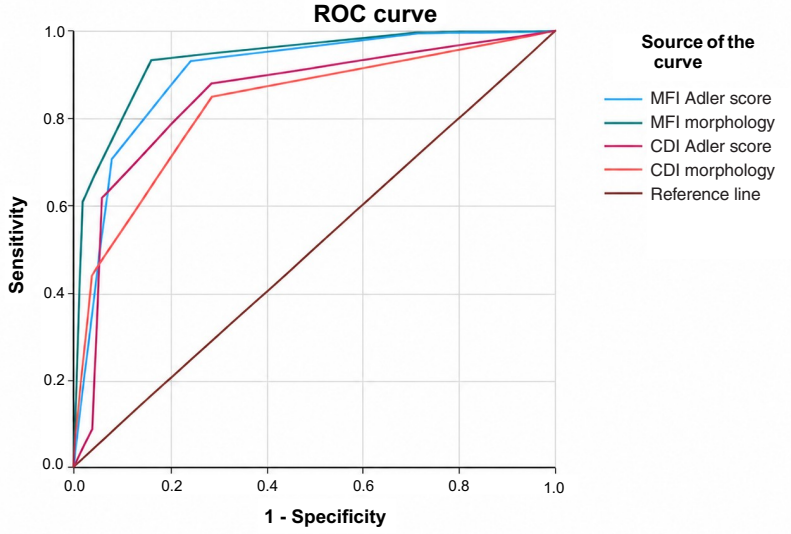
Variable	OR (95% CI)	P-value
MFI Adler score	1.72 (0.54–5.48)	0.360
MFI morphology score	6.13 (2.02–18.56)	0.001
CDI Adler score	2.12 (0.50–9.03)	0.308
CDI morphology score	0.38 (0.07–1.99)	0.251

OR, odds ratio; CI, confidence interval; MFI, microflow imaging; CDI, color Doppler imaging.

Discussion

This study compared conventional CDI and MFI for evaluating the vascular characteristics of peripheral lung lesions. The main finding was that the MFI morphology score provided the strongest diagnostic performance for differentiating malignant from non-neoplastic lesions and was the only Doppler parameter that remained an independent predictor of malignancy in multivariable analysis. Although CDI- and MFI-based vascular parameters were significantly higher in malignant lesions, only morphology assessment with MFI retained statistical significance after adjustment for the other Doppler variables. These findings suggest that detailed assessment of vascular architecture with MFI may add diagnostic information beyond conventional Doppler evaluation.

Malignant tumors are characterized by tumor-driven angiogenesis, which produces irregular and chaotic vascular architecture [10]. Conventional CDI may not adequately depict these microvascular structures because wall-filtering and motion-suppression mechanisms can eliminate slow-flow signals along with tissue-motion artifacts [11]. This limitation is particularly relevant in thoracic applications, where respiratory motion and lesion depth may further reduce Doppler sen-



Test result variables	Area	Std. Error	P	Asymptotic 95% confidence interval	
				Lower bound	Upper bound
MFI Adler score	0.899	0.031	<0.001	0.838	0.960
MFI morphology	0.933	0.023	<0.001	0.888	0.979
CDI Adler score	0.847	0.038	<0.001	0.772	0.922
CDI morphology	0.828	0.038	<0.001	0.754	0.902

Fig. 2. **Receiver operating characteristic (ROC) curves of Doppler parameters for differentiating malignant from non-neoplastic peripheral lung lesions.** MFI, microflow imaging; CDI, color Doppler imaging.

Table 4. Diagnostic performance of Doppler parameters in differentiating malignant from non-neoplastic peripheral lung lesions

Parameter	AUC (95% CI)	Cutoff	Sensitivity (%)	Specificity (%)
MFI morphology score	0.933 (0.888–0.979)	≥ 3	94	83
MFI Adler score	0.899 (0.838–0.960)	≥ 2	94	75
CDI Adler score	0.847 (0.772–0.922)	≥ 1	88	71
CDI morphology score	0.828 (0.754–0.902)	≥ 2	86	71

AUC, area under the curve; CI, confidence interval; MFI, microflow imaging; CDI, color Doppler imaging.

sitivity [2,12]. By improving separation of slow-flow vascular signals from background tissue motion, MFI may enable clearer visualization of intralesional microvascular patterns and more closely reflect the vascular features of tumor biology [11].

A second important finding was that morphology-based assessment outperformed semiquantitative vascular grading with the Adler score. The Adler grading system reflects the amount of detectable vascular signal but does not fully capture the spatial organization or architectural complexity of intralesional vessels [8]. Malignant angiogenesis is characterized not only by greater vascular density but also by structural abnormalities, including tortuosity, irregular branching, and chaotic distribution [13]. Accordingly, morphology-based evaluation may better represent tumor-specific vascular remodeling than simple vessel counts or signal-intensity grading [14]. In this cohort, that distinction may explain why the MFI morphology score remained an independent predictor of malignancy, whereas vascular grading parameters did not.

Although data on MFI in peripheral lung lesions remain limited, studies in other solid organs have reported improved microvascular detection and clearer vascular morphology delineation with microflow-based techniques than with conventional CDI [11]. In breast imaging, contrast-enhanced microflow techniques have improved characterization of vascular patterns in malignant masses [4]. Microflow pattern analysis has also been reported to help differentiate benign from malignant thyroid nodules [5]. Multiparametric ultrasound approaches that incorporate advanced vascular assessment have shown promise in axillary lymph node evaluation [6], and studies of renal tumors have reported improved diagnostic performance with MFI [9]. The present findings extend these observations to pleura-based lung lesions and suggest that morphology-based microvas-

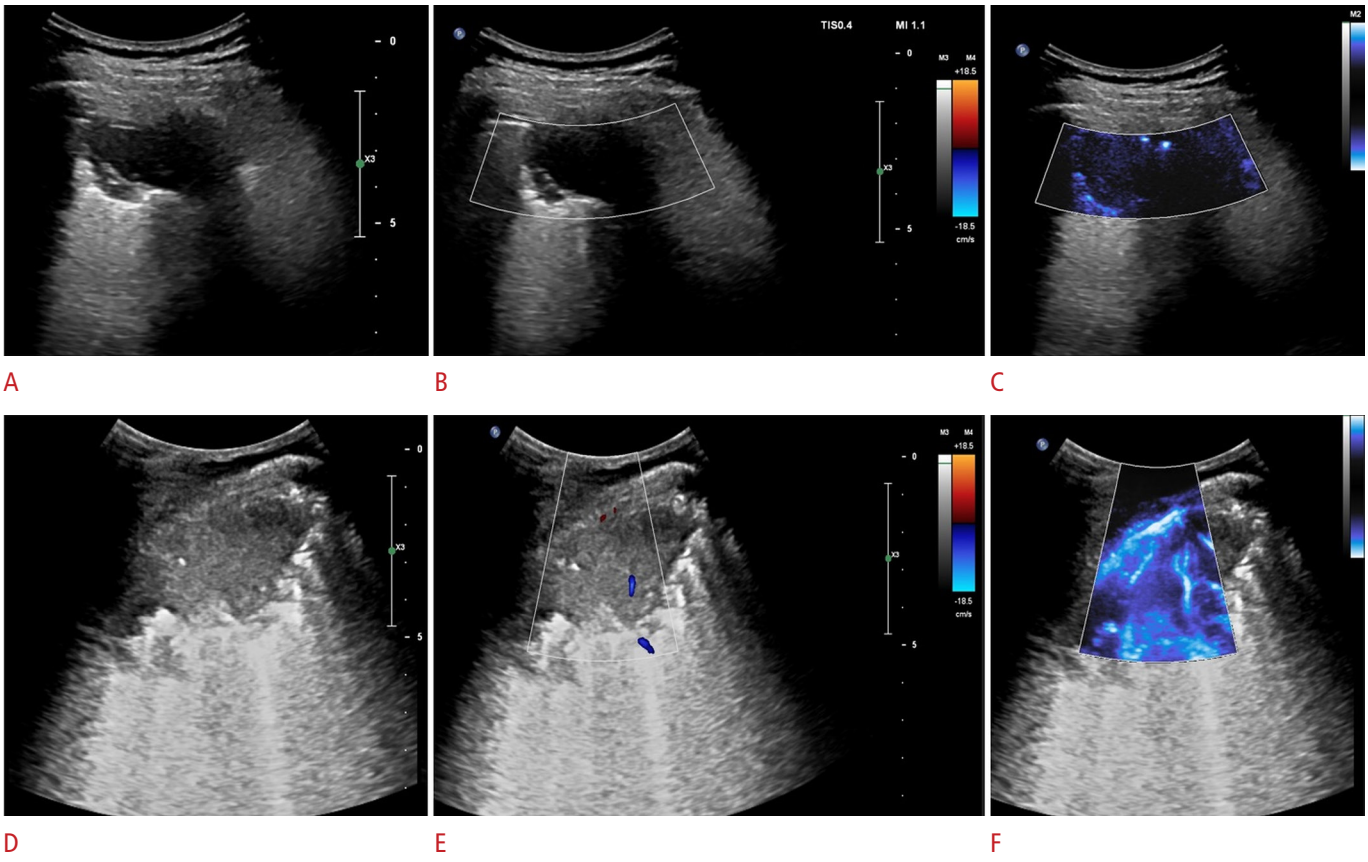


Fig. 3. Comparison of color Doppler imaging and microflow imaging in non-neoplastic and malignant peripheral lung lesions.
A–C. Peripheral lung lesion in a 72-year-old woman was diagnosed with a non-neoplastic inflammatory/infectious lesion. A. B-mode ultrasound demonstrates a 38-mm subpleural hypoechoic solid lesion. B. Color Doppler imaging shows no detectable intralesional vascular signal (Adler score 0; type I morphology). C. Microflow imaging reveals minimal punctate intralesional vascular signals (Adler score 1; type II morphology) without peripheral rim-like or chaotic vascular architecture. Histopathological examination confirmed a non-neoplastic inflammatory/infectious lesion. D–F. Peripheral lung adenocarcinoma was diagnosed in a 65-year-old man. D. B-mode ultrasound shows a 65-mm subpleural hypoechoic solid lesion. E. Color Doppler imaging demonstrates moderate intralesional vascularity (Adler score 2; type III morphology). F. Microflow imaging reveals markedly increased and disorganized intralesional vascularity with peripheral and chaotic vascular patterns (Adler score 3; type V morphology). Histopathological examination confirmed adenocarcinoma.

cular assessment may be informative in this anatomical setting.

In thoracic imaging, ultrasound has an established role in evaluating and guiding biopsy of peripheral lung lesions [1–3]. Although CEUS can be used to assess lung-lesion perfusion characteristics [7], it is a separate modality with higher cost and limited availability in routine practice. MFI, in contrast, can be added to standard thoracic ultrasound examinations without contrast administration and may improve vascular assessment within routine workflows.

Clinically, the findings indicate that higher MFI morphology scores are strongly associated with malignancy and may help stratify risk in patients with peripheral lung lesions. Lesions with disorganized or chaotic intralesional vascular patterns on MFI were highly suggestive of malignant pathology, whereas lesions with absent or minimal vascular architecture were more often non-neoplastic. Imaging findings cannot replace histopathological confirmation, but morphology-based MFI assessment may improve noninvasive risk stratification and help inform decisions about biopsy or follow-up when incorporated into routine thoracic ultrasound evaluation.

Several limitations should be acknowledged. First, the retrospective single-center design may limit generalizability. Second, all ultrasound examinations were performed by a single experienced operator; this promoted technical consistency but may restrict external reproducibility. Third, power Doppler imaging was not included in the study protocol. Fourth, although MFI morphology types were analyzed as an ordinal variable, biological overlap between adjacent morphology patterns may occur in clinical practice, particularly in inflammatory non-neoplastic lesions. Nevertheless, cross-tabulation analysis (Supplementary Table 1) showed a progressive increase in

the proportion of malignant lesions from type I (0.0%) to type V (97.9%), with a significant linear trend across morphology categories (linear-by-linear association, $P<0.001$). These findings support use of the ordinal morphology classification for ROC analysis in this cohort, despite the potential for clinical overlap. Finally, although malignant subtypes were recorded, subtype-specific vascular pattern analysis was beyond the primary scope of this study. Prospective multicenter studies with larger cohorts are needed to validate these findings and clarify the role of MFI in thoracic ultrasound.

In conclusion, the MFI morphology score performed better than conventional color Doppler parameters for differentiating malignant from non-neoplastic peripheral lung lesions and remained an independent predictor of malignancy. Detailed assessment of vascular architecture, rather than vascular quantity alone, appears to better reflect tumor-related angiogenesis in pleura-based lung lesions. Incorporating MFI morphology evaluation into routine thoracic ultrasound may improve noninvasive risk stratification and support clinical decision-making. Prospective multicenter studies are needed to confirm these findings and define the role of MFI in thoracic applications.

ORCID

Mustafa Yeşilyurt: https://orcid.org/0000-0002-7605-4940
Ahmet Tuğrul Akkuş: https://orcid.org/0000-0001-5269-2502
Buğra Kerget: https://orcid.org/0000-0002-6048-1462
Fahri Aydin: https://orcid.org/0000-0003-0918-9666
Adem Karaman: https://orcid.org/0000-0002-3091-0609
Fatih Alper: https://orcid.org/0000-0002-9483-8861

Author Contributions

Conceptualization: Yeşilyurt M. Data acquisition: Yeşilyurt M, Akkuş AT, Aydin F, Karaman A. Data analysis or interpretation: Akkuş AT, Kerget B, Alper F. Drafting of the manuscript: Yeşilyurt M, Aydin F. Critical revision of the manuscript: Akkuş AT, Kerget B, Karaman A, Alper F. Approval of the final version of the manuscript: all authors.

Conflict of Interest

No potential conflict of interest relevant to this article was reported.

Supplementary Material

Supplementary Table 1. Cross-tabulation of MFI morphology types I–V according to the final diagnosis (https://doi.org/10.14366/usg.26073).

References

1. Zhao ZL, Peng LL, Wei Y, Li Y, Wang GM, Yu MA. The accuracy of ultrasound-guided lung biopsy pathology and microbial cultures for peripheral lung lesions. J Thorac Dis 2020;12:858-865.
2. Hendin A, Koenig S, Millington SJ. Better with ultrasound: thoracic ultrasound. Chest 2020;158:2082-2089.
3. Huang W, Chen L, Xu N, Wang L, Liu F, He S, et al. Diagnostic value and safety of color doppler ultrasound-guided transthoracic core needle biopsy of thoracic disease. Biosci Rep 2019;39:BSR20190104.
4. Luo R, Wang Q, Zhang Y, Jiang W, Wang Y, Luo Y. Value of contrast-enhanced microflow imaging in diagnosis of breast masses in comparison with contrast-enhanced ultrasound. Acad Radiol 2024;31:2217-2227.
5. Li W, Gao L, Du Y, Wang Y, Yang X, Wang H, et al. Ultrasound microflow patterns help in distinguishing malignant from benign thyroid nodules. Cancer Imaging 2024;24:18.
6. Dobruch-Sobczak K, Szlenk A, Gumowska M, Maczewska J, Fronczewska K, Lukasiewicz E, et al. Multiparametric ultrasound assessment of axillary lymph nodes in patients with breast cancer. Sci Rep 2024;14:23072.
7. Jimenez-Serrano S, Paez-Carpio A, Domenech-Ximenos B, Cornellas L, Sanchez M, Revzin MV, et al. Conventional and contrast-enhanced US of the lung: from performance to diagnosis. Radiographics 2024;44:e230171.
8. Adler DD, Carson PL, Rubin JM, Quinn-Reid D. Doppler ultrasound color flow imaging in the study of breast cancer: preliminary findings. Ultrasound Med Biol 1990;16:553-559.
9. Li C, Qi L, Geng C, Xiao H, Wei X, Zhang T, et al. Comparative diagnostic performance of color Doppler flow imaging, MicroFlow imaging and contrast-enhanced ultrasound in solid renal tumors. Acad Radiol 2025;32:3475-3484.
10. Mou J, Li C, Zheng Q, Meng X, Tang H. Research progress in tumor angiogenesis and drug resistance in breast cancer. Cancer Biol Med 2024;21:571-585.
11. Aziz MU, Eisenbrey JR, Deganello A, Zahid M, Sharbidre K, Sidhu P, et al. Microvascular flow imaging: a state-of-the-art review of clinical use and promise. Radiology 2022;305:250-264.
12. Colares PF, Mafort TT, Sanches FM, Monnerat LB, Menegozzo CA, Mariani AW. Thoracic ultrasound: a review of the state-of-the-art. J Bras Pneumol 2024;50:e20230395.
13. Lugano R, Ramachandran M, Dimberg A. Tumor angiogenesis: causes, consequences, challenges and opportunities. Cell Mol Life Sci 2020;77:1745-1770.
14. Sladkevicius P, Jokubkiene L, Timmerman D, Fischerova D, Van Holsbeke C, Franchi D, et al. Vessel morphology depicted by three-dimensional power Doppler ultrasound as second-stage test in adnexal tumors that are difficult to classify: prospective diagnostic accuracy study. Ultrasound Obstet Gynecol 2021;57:324-334.